Research Article

Rouhina Saemi, Elham Taghavi, Hoda Jafarizadeh-Malmiri, and Navideh Anarjan*

Fabrication of green ZnO nanoparticles using walnut leaf extract to develop an antibacterial film based on polyethylene–starch–ZnO NPs

https://doi.org/10.1515/gps-2021-0011
received September 29, 2020; accepted December 27, 2020

Abstract: Zinc oxide nanoparticles (ZnO NPs) were synthesized utilizing prepared walnut leaf extract by various amounts of its leaves (5–25 g) via a heater and stirrer adjusted at 60°C and reaction time ranging from 30 to 90 min. Fourier transform infrared spectroscopy and gas chromatography indicated the six main functional groups and 29 bioactive compounds in the provided walnut leaf extract. Antioxidant and antibacterial inhibitory activities of the fabricated ZnO NPs, in powder form, were modeled as a function of two synthesized parameters using response surface methodology, and the fabrication process was optimized. The results indicated that the ZnO NPs synthesized using walnut leaf extract, with 15.51 g of its dried powder and reaction time of 60 min, had maximum antioxidant activity and antibacterial effects against *Escherichia coli*. X-ray diffraction analysis and scanning electron microscopy image indicated that the synthesized ZnO NPs using optimal processing conditions had crystals in triangular nanoprisms to nearly spherical shape with the particle size ranging from 15 to 40 nm. Finally, prepared biodegradable film composed of thermoplastic starch (5% w/w), polyethylene (93% w/w), and ZnO NPs (2% w/w) indicated high bactericidal inhibitory activity against both Gram-positive (*Staphylococcus aureus*) and Gram-negative (*E. coli*) bacterial strains.

Keywords: antioxidant activity, antimicrobial activity, green synthesis, packaging, zinc oxide nanoparticles

*** Corresponding author: Navideh Anarjan,** Department of Engineering, Tabriz Branch, Islamic Azad University, East Azarbaijan, Tabriz, Iran, e-mail: anarjan@gmail.com
Rouhina Saemi: Department of Engineering, Tabriz Branch, Islamic Azad University, East Azarbaijan, Tabriz, Iran
Elham Taghavi: Faculty of Fisheries and Food Science, Universiti Malaysia Terengganu, 21030, Kuala Nerus, Terengganu, Malaysia
Hoda Jafarizadeh-Malmiri: Department of Food Engineering, Faculty of Chemical Engineering, Sahand University of Technology, Tabriz, Iran; Department of Food Science and Technology, Applied Scientific Training Center of Shirin Asal Food Industries Group, Tabriz, Iran

1 Introduction

Recently, the field of nanotechnology has attracted interest particularly due to the synthesis of nanoparticles (NPs) and applications in different fields such as nutrition, energy, and pharmacological industry and engineering sciences. These numerous applications of NPs can be related to their high surface area [1–4]. This aspect has attracted numerous researchers to find novel methods for the synthesis NPs without any toxic chemical materials. Biosynthesis methods for NPs synthesis via enzymes, microorganisms, and plant extracts have more advantage over other chemical and physical synthesis procedures [4–6]. Currently, a variety of researches have been conducted on the synthesis of metal NPs using various metal ions (e.g., Au, Pd, Ag, and Pt) and plant extracts as reducing agents [1,7–9]. Green synthesis of CuO, TiO_2, MgO, and ZnO using plant extracts has been reported for their antibacterial activity properties [10–15].

Plants extracts containing reducing and stabilizing agents provide a biological synthesis path of metallic NPs without using toxic organic solvents, which allows a controlled synthesis with highly ordered NPs of any size, shape, and dispersion [2,16]. Several plants such as *Aloe vera*, *Geranium*, strawberry, and walnut and their derivatives containing leaf, stem, and flower have been used in metal NPs synthesis. Walnut leaves are natural, easily available, and of low cost [17–20]. Also, walnut leaves contain a wide range of biologically active compounds such as being rich in naphthoquinones and flavonoids, and those are considered as major flavonols and phenolic compounds [20,21]. Free radicals show the existence of the extra number of electrons, and accordingly, those are vastly active compound and have electrical charge. It has been known that phenolic compounds

are considered as a class of antioxidant agent, which can also protect by acting as free radical scavengers [22–24]. Walnut leaves have also functional properties such as antimicrobial, antifungal, anti-inflammatory, antioxidant, antidiarrheic, antihelmintic, depurative, and astringent [20,22,25,26]. Furthermore, walnut leaves have reducing and stabilizing activities due to their biomolecules such as phenolic compounds, flavonoids, proteins, and carbohydrates, which are able to reduce metal ions and produce the metal oxide nanoparticles with an aqueous medium while steering clear of the presence of toxic substance and solvents [27,28].

Among the inorganic NPs, ZnO NPs receive specific attention because they are low cost, easily available, and safe. They have properties such as semiconducting, unique antibacterial, wound healing, antifungal, UV filtering properties, exclusive catalytic optical, electronic, magnetic, and photochemical activities [13,29–31]. ZnO NPs is a band gap oxide semiconductor of about 3.37 eV at room temperature with high excitation binding energy of about 60 meV [16,32]. In the recent decades, several researches have been done on the synthesis of metal NPs utilizing plant extracts. To the best our insight, ZnO NPs have not been synthesized using the walnut leaf extract. However, some studies have been performed on the synthesis of other metal NPs such as silver NPs using the walnut leaf extract [33].

The current study depicts green and rapid synthesis method and characterization of synthesized ZnO NPs by biological (green) techniques using the walnut leaf extract. In addition to the chemical and physical properties, antioxidant and antimicrobial activities of the synthesized ZnO NPs were investigated using the response surface methodology (RSM). Finally, the optimal ranges and optimal conditions for the synthesis of NPs were determined, and the synthesized NPs have been used in the composition of a packaging film based on polyethylene and starch.

2 Materials and methods

2.1 Materials

Walnut leaves were obtained from local gardens of Tabriz, Iran. $Zn(NO_3)_3{\cdot}6H_2O$ was bought from Merck (Merck GmbH & Co. KG, Darmstadt, Germany). DPPH (2,2-diphenyl-2-picrylhydrazyl) was purchased from Sigma Company (St. Louis, Missouri, USA). *Escherichia coli* (PTCC 1270) and *Staphylococcus aureus* (PTCC 1112) were purchased from Microbial Persian Type Culture Collection (PTCC, Tehran, Iran). Nutrient agar (NA) was acquired from Biolife (Biolife Co. Milan, Italy). Low-density polyethylene (LDPE) and glycerol were bought from Petrochemical Industries of Iran. Starch was prepared from Glucosan Company (Qazvin, Iran). Deionized double distilled water (DI) was purchased from Dr. Mojallali Chemical Complex Co. (Tehran, Iran).

2.2 Preparation of plant extraction

Preparation of the leaf extract is one of the major activity. Fresh leaves of walnut were cleaned by washing greatly 2–3 times with water and by double distilled water afterward to eliminate any dirt and impurity. Then, leaves were dried in the shade at ambient temperature for 14 days to totally wipe out the dampness. The obtained dried leaves, by utilizing domestic miller (MX-GX1521, Panasonic, Tokyo, Japan), were powdered.

Briefly, various amounts of dried walnut leaves powder (5–25 g) were weighed and mixed in 50 mL of bubbling DI double distilled water for 30 min at 60°C. This mixture was filtered via Whatman No. 40 filter paper. The subsequent walnut extract was kept at the temperature of 4°C in the refrigerator (Figure 1a).

2.3 Synthesis of ZnO nanoparticles

In a typical synthesis, 2 g $Zn(NO_3)_3{\cdot}6H_2O$ was dissolved in 20 mL of the walnut leaf extract and volume up to 50 mL by DI double distilled water. The solution was placed on a stirrer at 60°C for various duration (30–90 min). The prepared solution was heated in a furnace at 400°C for 2 h. Finally, white colored powder (thermally dehydrates ZnO NPs, Figure 1b) was obtained. This powdered product was utilized for further investigation.

2.4 Physicochemical analyses

The chemical composition of the walnut leaves extract was analyzed utilizing a Fourier transform infrared spectroscopy (FTIR) (Bruker tensor 27-Germany) and GC-MS (Agilent 6890, Santa Clara, CA). The fabricated ZnO NPs were characterized by X-ray diffractometry (XRD; D5000, Siemens) utlizing Cu Kα radiation and scanning electron microscopy (SEM; mv 2300, Com scan) for assessing the

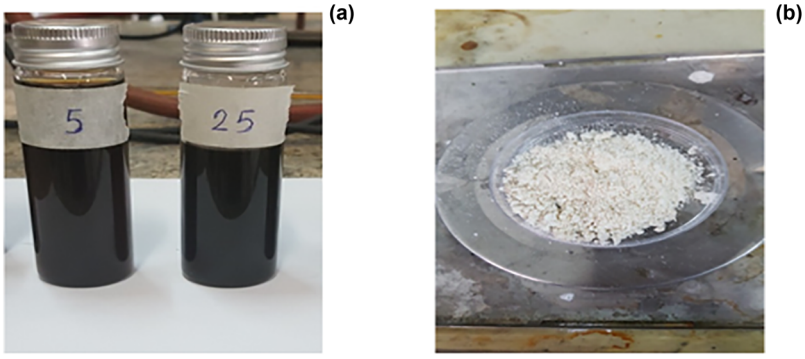

Figure 1: Walnut leaf extract (a) and synthesized ZnO NPs (b).

structural properties. The measurements of UV-visible spectroscopy (250–800 nm, Jenway 6705-USA) were performed to determine the antioxidant activity.

2.5 Antibacterial assay synthesized ZnO NPs

To evaluate the antibacterial property of fabricated ZnO NPs, the effect of NPs on the suspensions of bacterial was examined. The examination of the antibacterial activity was carried out through the well diffusion method. In fact, the bacterial species were inoculated on Nutrient Agar (NA Merck, Germany) plate (90 mL in diameter) and incubated for 18–24 h at 37°C. Three to five well-isolated colonies of the same morphological type were mixed in 10–15 mL of sterile normal saline solution. The bacterial suspension density was adjusted to 0.5 McFarland standard. This is equivalent to 1.5×10^8 colony-forming units of bacteria in 1 mL of prepared inoculums. A total of 0.1 mL of this bacterial suspension was spread on the surface of the solid NA plates, and a hole, with a diameter of 5 mm, was made on the solid agar. Then, ZnO NPs were poured into the holes and incubated at 37°C for 24 h. The antibacterial activity of the synthesized ZnO NPs was correlated with the diameter of the clear zone around the holes. Ampicillin disc with a diameter of 5 mm (Oxoid, 10 µg/disc) was used as a positive control for both Gram-positive and Gram-negative bacterial strains, and the antibacterial activity of the synthesized ZnO NPs was compared to the ampicillin and presented.

2.6 Determination of antioxidant activity

The ability of scavenging of ZnO NPs on DPPH was measured according to the method reported earlier by Sayyar and Jafarizadeh-Malmiri [12]. In this method, various concentrations of ZnO NPs were added into 1 mL of methanol (50%) solution containing DPPH (1 mM). Then, the mixture was shaken strongly and left to stand for 30 min in the dark before measuring the absorbance at 520 nm against a blank. Eq. 1 was applied to calculate the antioxidant activity:

$$I\% = (A_{\text{control}} - A_{\text{sample}})/A_{\text{control}} \times 100, \quad (1)$$

where $I\%$ is defined as the inhibition percent, A_{control} is the absorbance of the control reaction (including methanol and DPPH), and A_{sample} is the absorbance of the test compound.

2.7 Experimental design and statistical analysis

Response surface methodology (RSM) utilizing a central composite design (CCD) using two independent variables (synthesis factors), namely, the amount of dried walnut leaf powder (5–25 g) (X_1) and time of reaction (30–90 min) (X_2), was carried out to specify the antioxidant activity (Y_1) and the antibacterial activity (Y_2) of the ZnO NPs.

Comparing with other types of experimentation techniques, which are proven on classical one-variable-at-a-time optimization, RSM has numerous advantages. For instance, a large amount of information can be generated from a small number of experiments. Also, the ability to assess the interaction of the independent variables with the response variable is another advantage of RSM. Therefore, it could be utilized to optimize the main independent factors of the process to achieve a product with desired characters [34,35]. Hence, 13 runs of experiment that have five central points were created via utilizing the software Minitab v.16 statistical package (Minitab Inc., PA, USA) [36]. All experiments were conducted through a day via utilizing one block. A second-order polynomial equation

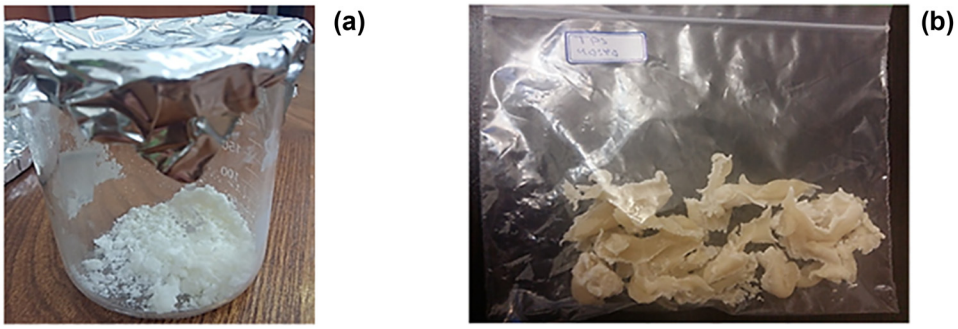

Figure 2: Mixture of starch and glycerol (a) and thermoplastic starch (b).

(Eq. 2) was applied to correlate the Y_1 and Y_2 of the ZnO NPs solution with the studied synthesis variables.

$$Y = a_0 + a_1X_1 + a_2X_2 + a_{11}X_1^2 + a_{22}X_2^2 + a_{12}X_1X_2, \quad (2)$$

where a_0 is a constant and a_i, a_{ii}, and a_{ij} are corresponded to the linear, quadratic, and interaction effects, respectively. The appropriateness of the model was tested accounting for the coefficient of determination (R^2) and adjusted coefficient of determination (R^2-adj). Furthermore, analysis of variance (ANOVA) was used to provide the important determinations of the concluded models in terms of p-value. Small p-value (<0.05) was viewed as significant in terms of statistic. To predict the interactions of independent variable, three-dimensional surface plots and two-dimensional contour plots were plotted based on the fitted polynomial equations [36].

Numerical multiple response and graphical optimizations were applied to achieve the optimum values for independent variable with the desired response variables [37]. Via estimating the resulted surface plots, optimal conditions for the independent factors were acquired. Finally, three additional endorsement examinations were performed at optimum synthesis conditions used for verification of the validity of the statistical experimental approaches. Therefore, it is a suitable method that could be utilized to optimize the main independent factors of the process [37,38].

2.8 Preparation of film

2.8.1 Preparation of thermoplastic starch

To prepare the thermoplastic starch, starch was placed in the vacuum oven to dry completely for 24 h at 80°C (Figure 2a). Then, dried starch was mixed with glycerol with weight percent (wt%) of 65% starch and 35% glycerol. Finally, raw materials were mixed using a blender at 110°C for 15 min and 30 rpm (Figure 2b).

2.8.2 Process of preparing polyethylene–starch–ZnO nanoparticles nanocomposite

To prepare nanocomposite, thermoplastic starch and polyethylene of about 5 wt% and 95 wt%, respectively, were mixed at 160°C for 5 min and 60 rpm. Finally, ZnO nanoparticles of about 2 wt% was added (Figure 3a). At the end, mixture was preheated at 170°C for 5 min. Then to shape, mixture was placed under pressure of 50 bar

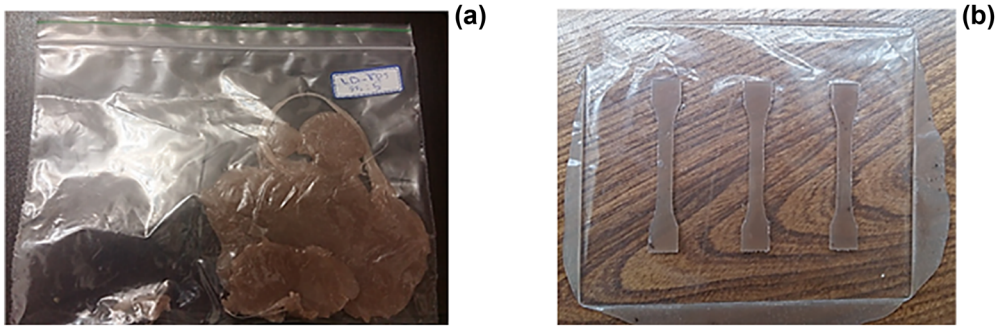

Figure 3: Polyethylene–starch–ZnO nanoparticles nanocomposite (a) and dumbbell shape of mixture (b).

and 170°C for 5 min and then cooled at the same pressure to 50°C. Figure 3b shows the obtained dumbbell shape of mixture.

2.8.3 Antibacterial assay of polyethylene–starch–ZnO film

To assess bacterial activity of polyethylene–starch–ZnO NPs film, the effect of the film on the prepared bacterial was assessed for both Gram-positive (*S. aureus*) and Gram negative (*E. coli*). The bacterial species was inoculated on Nutrient Agar (NA Merck, Germany) media, and then some wells were made on media. Polyethylene–starch–ZnO films were separately positioned in the wells. Plates were placed in an incubator at 37°C for 24 h.

3 Results and discussion

3.1 Extract specifications (FTIR analysis)

The FT-IR examination was carried out to recognize the possible biomolecules of walnut leaves responsible for the synthesis of ZnO nanoparticles. The FT-IR spectrum of the extract of walnut leaves (Figure 4) revealed some peaks at 2,921, 2,356, 1,569, 1,457, 1,305, and 674 cm^{-1}, which represent a carboxylic acid group (C–O), P–H phosphine strength, C═N amine strength, C═C aromatic stretching vibrations, carbonyl group (C═O), and C-Br alkyl halide stretching, respectively [39]. These peaks recommended the presence of regenerative material such as carboxylic acid and aromatic ester compounds in the plant extract, which could be in charge for the reduction of metal oxide ions and formation of the corresponding metal oxide nanoparticles. Sheikhlou et al. could successfully synthesis selenium NPs using walnut leaf extract, and they found that amid groups existed in the walnut extract, which were related to the proteins and enzymes, had a key role in the reduction of ions [40].

3.2 GC-MS analysis of walnut leaves

To understand exactly regenerative compounds, GC-MS analysis was performed in the walnut leaves, which were in charge of the synthesis of ZnO NPs (Figure 5). It was found that within 63 min of retention time, approximately 29 active compounds were found. However, five noticeable compounds were found at different chromatogram peaks. They are monoterpenes hydrocarbons, esters, alcohol, terpene hydrocarbons, and oxygen terpene that might influence the stability of the formed ZnO NPs and the reduction process (Table 1).

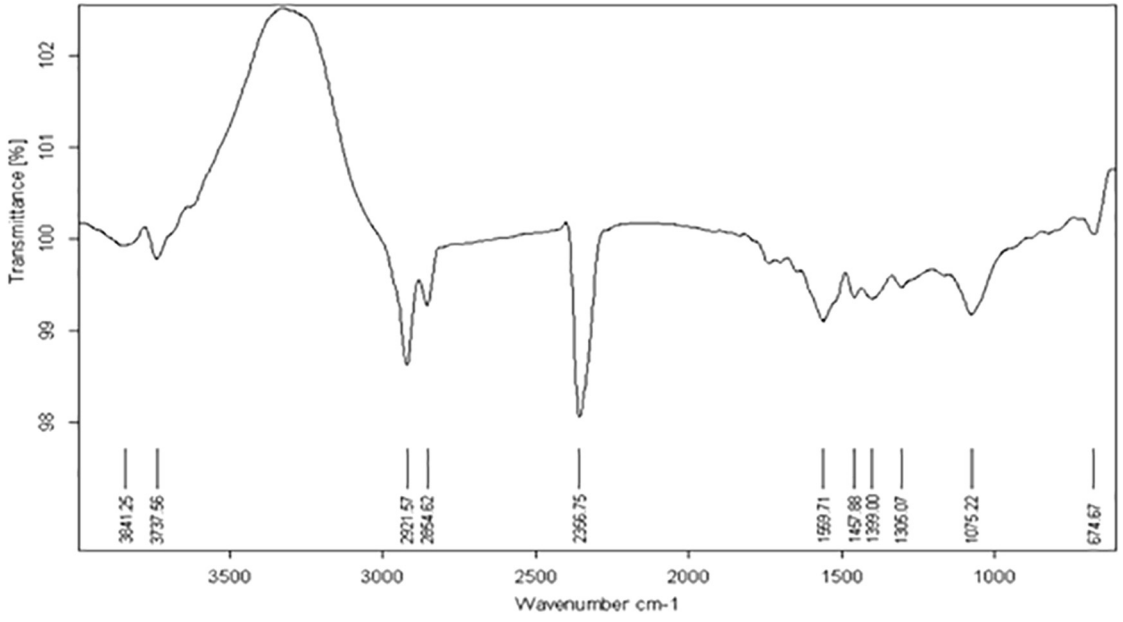

Figure 4: FT-IR spectrum of walnut leaf extract.

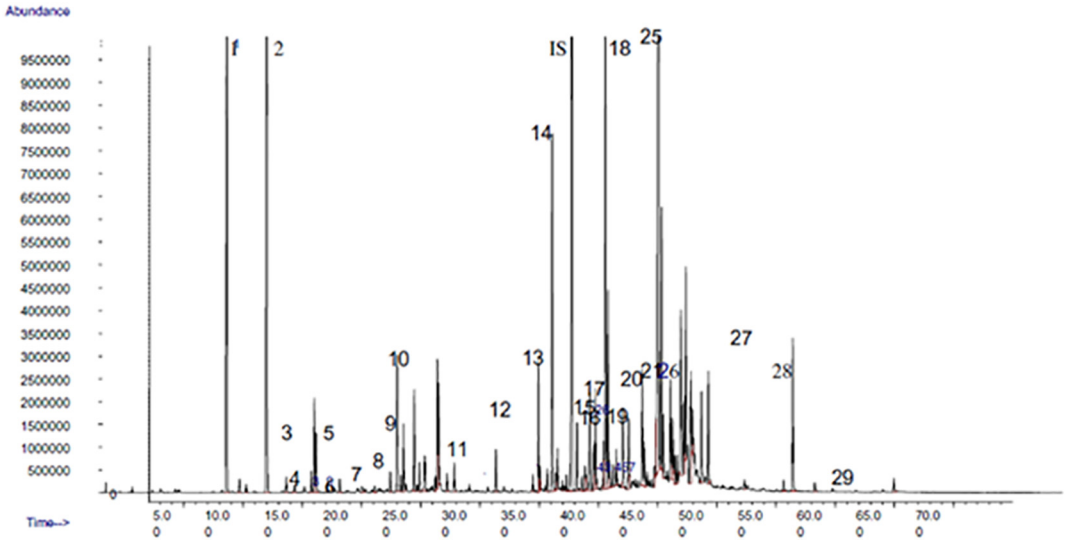

Figure 5: GC-MS analysis of walnut leaves.

3.3 Fitting the response surface models

By using designed experiments, as presented in Table 2, and through applying multiple regression analysis, second-order polynomial models for studying two ZnO NPs synthesis factors were fitted. Both the estimated regression coefficients and the corresponding significance of regressions for the models are presented in Table 3.

The p-value of all the main, quadratic, and interaction terms of the achieved final models are presented in Table 4. Commonly, the lesser p-value is important for the elected term on the responses. High values of the R^2 and R^2-adj for the achieved models showed a good measure for the overall accuracy and performance of the models. Furthermore, the accomplished insignificant lack of fits for attained models established their sufficient fitness for the effects of the synthesis factor (Table 3).

The main terms of the synthesis variables, as presented in Table 4, had a significant ($p < 0.05$) effect on all responses of the formed ZnO NPs. The gained results showed that the main term of the amount of reaction time (X_2) had the most significant ($p < 0.05$) effect on antibacterial and antioxidant activities of the formed ZnO NPs. However, dried powder (X_1) was not the effective factor

Table 1: GC-MS analysis of walnut leaves

Compounds	No.	Area (%)	Time (min)	Compounds	No.	Area (%)	Time (min)
α-Pinene	1	6.5	10	*Geranyl acetate*	16	1	42
β-Pinene	2	9.5	15	*β-Farnesene*	17	1	43
β-Myrcene	3	0.1	16	*Y-Muurolene*	18	0	45
Cymene	4	0.2	17	*Germacrene*	19	6	46
Limonene	5	1	18	*Curcumene*	20	2	47
1.8-Cineol	6	0.7	19	*y-Amorphene*	21	0	47
α-Terpinene	7	0.1	21	*α-Murrolene*	22	0	47
Terpinolene	8	0.1	24	*y-Muurolene*	23	1	47
Camphor	9	0.2	25	*y-Cadinene*	24	1	47
Myrtenol	10	0.2	25	*Caryophyllene oxide*	25	18	48
Bornyl acetate	11	0.4	31	*Valen cene*	26	2.2	49
Eugenol	12	0.2	34	*Agrospiol*	27	1.8	55
β-Bourbounene	13	3.9	37	*α-Eudesmol*	28	1.9	59
β-Caryophyllene	14	12.8	39	*Manool*	29	0.4	63
α-Humelene	15	1	41				

Table 2: Experimental runs based on the central composite design and response variables for ZnO NPs synthesis

Sample number	Amount of dried powder (g) X_1	Reaction time (min) X_2	Antibacterial (mm) Y_1		Antioxidant (%) Y_2	
			Exp[a]	Pre[b]	Exp[a]	Pre[b]
1	7.9	39	8	7.7	14.7	15.7
2	25.0	60	9	8.3	16.8	16.6
3	22.0	81	7	7.0	19.3	20.3
4	15.0	30	8	8.1	18.6	18.4
5	15.0	60	8	9.0	26.0	26.3
6	15.0	60	9	9.0	27.6	26.3
7	15.0	60	9	9.0	28.1	26.3
8	22.0	39	9	8.9	17.7	17.4
9	5.0	60	8	8.1	16.8	14.8
10	15.0	60	9	9.0	25.0	26.3
11	15.0	60	9	9.0	25.0	26.3
12	7.9	81	8	7.9	17.3	19.5
13	15.0	90	7	6.9	25.0	23.1

[a] Experimental values of studied responses. [b] Predicted values of studied responses.

Table 3: Regression coefficients, R^2, R^2-adj, and probability values for the fitted models

Regression coefficient	Antibacterial (diameter of clear zone mm)	Antioxidant (%)
a_0 (constant)	−0.272	−27.20
a_1 (main effect)	0.433	3.358
a_2 (main effect)	0.218	0.845
a_{11} (quadratic effect)	−0.007	−0.105
a_{22} (quadratic effect)	−0.001	−0.006
a_{12} (interaction effect)	−0.003	−0.0016
R^2	97.75%	91.63%
R^2-adj	94.93%	85.66%

a_0 is a constant, and a_i, a_{ii}, and a_{ij} are the linear, quadratic, and interaction coefficients of the quadratic polynomial equation, respectively.

on antibacterial and antioxidant activities of ZnO NPs. The results also showed that the quadratic term of the reaction time and the amount of dried powder had a significant effect ($p < 0.05$) on all responses studied in the current research. In addition, the results showed that the interaction effect of independent factors had an insignificant effect on the mean antioxidant activity of the synthesized ZnO NPs but had a significant effect on the mean antibacterial activity of the formed ZnO NPs.

Table 4: *P*-value of the regression coefficients in the obtained models

		Antibacterial (Y_2) *P*-value	Antioxidant (Y_1) *P*-value
Main effects	X_1	0.508	0.361
	X_2	0.002	0.036
Quadratic effects	X_1^2	0.015	0.000
	X_2^2	0.001	0.005
Interacted effects	X_1X_2	0.005	0.79

3.3.1 Antibacterial activity of ZnO NPs

As illustrated in Table 2, the antibacterial inhibitory activity of the gained ZnO NPs against *E. coli* (zone of inhibition) varied from 7 to 9 mm for various samples. The changes in the range of the antibacterial inhibitory activity of ZnO NPs can be a result of both reaction time and the amount of dried powder as depicted in Figure 6a. As this figure shows, at a constant and low reaction time for the formed ZnO NPs, by increasing the amount of dried leave powder, the diameter of the shaped clear zone inhibition increased. The achieved results could

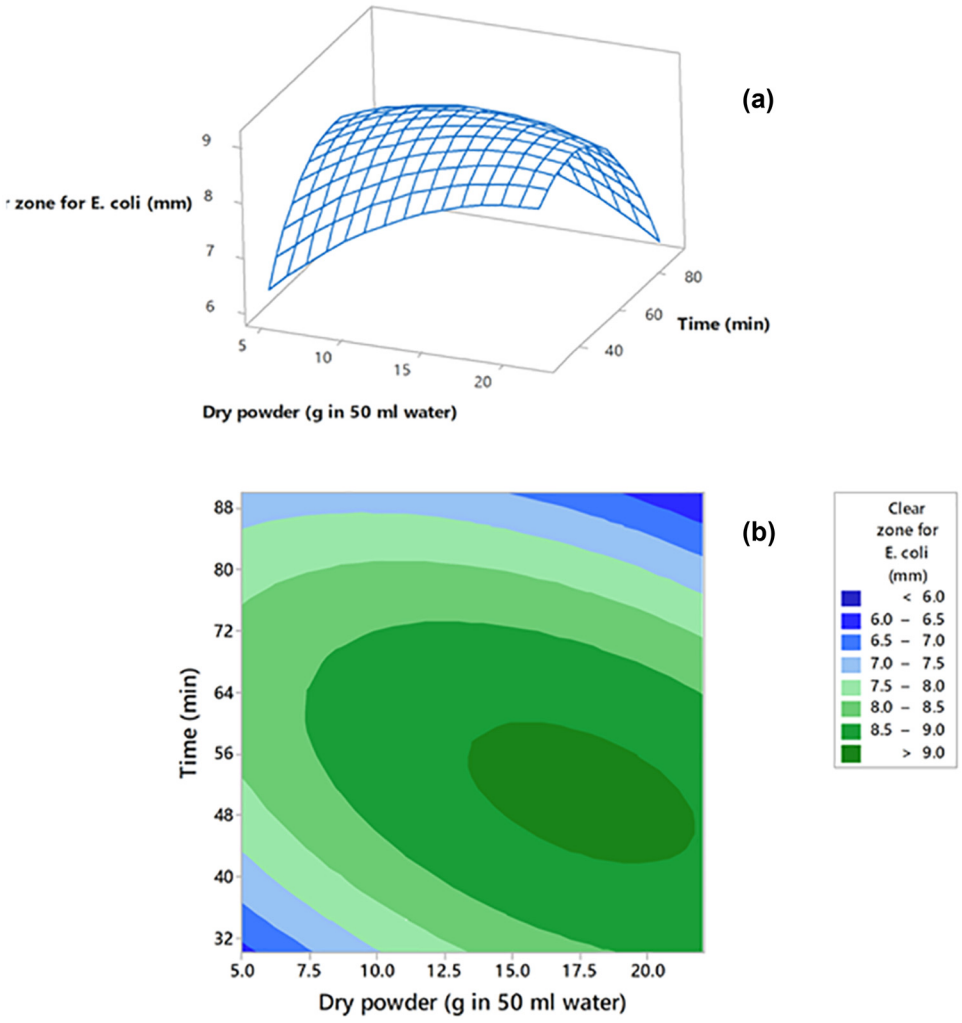

Figure 6: Response surface (a) and contour plots (b) for the antibacterial activity of ZnO NPs as function of significant ($p < 0.05$) interaction effects of reaction time and amount of dried powder.

be clarified by the way that by increasing the amount of walnut leaf extract, the concentration of the regenerative substances in the extract increased, which in turn increased the concentration of the formed ZnO NPs. However, at both constant and low amount of extract, there was an insignificant increase in the diameter of zone inhibition due to the low amount of regenerative agent ($p > 0.05$). Although the interaction of amount of extract and time of reaction had significant ($p < 0.05$) effect on the antibacterial property of the synthesized ZnO NPs. Obtained results also demonstrated that by increasing the reaction time at a constant and high amount of dried powder, the antibacterial inhibitory activity of the fabricated ZnO NPs decreased because regenerative agents destroy by increasing the reaction time. These results have led to high levels of agreement with the previous finding by Madan et al. [12]. Their finding showed that the concentration of green formed ZnO NPs and their antibacterial inhibitory properties increased via increasing the amount of extract of *Azadirachta indica*. As obviously illustrated in Figure 6b, the highest antibacterial properties of the fabricated ZnO NPs against *E. coli* was gained at a maximum amount of walnut leaf extract and low reaction time.

3.3.2 Antioxidant activity of synthesized ZnO NPs

Table 2 presents the antioxidant activity of the formed ZnO NPs, which varied from 14% to 28%. As results clearly showed, the ZnO NPs can be synthesized via utilizing natural regenerative agents in the extract of walnut leaves with no application of other chemical regenerative agents. Figure 7a shows the antioxidant property of

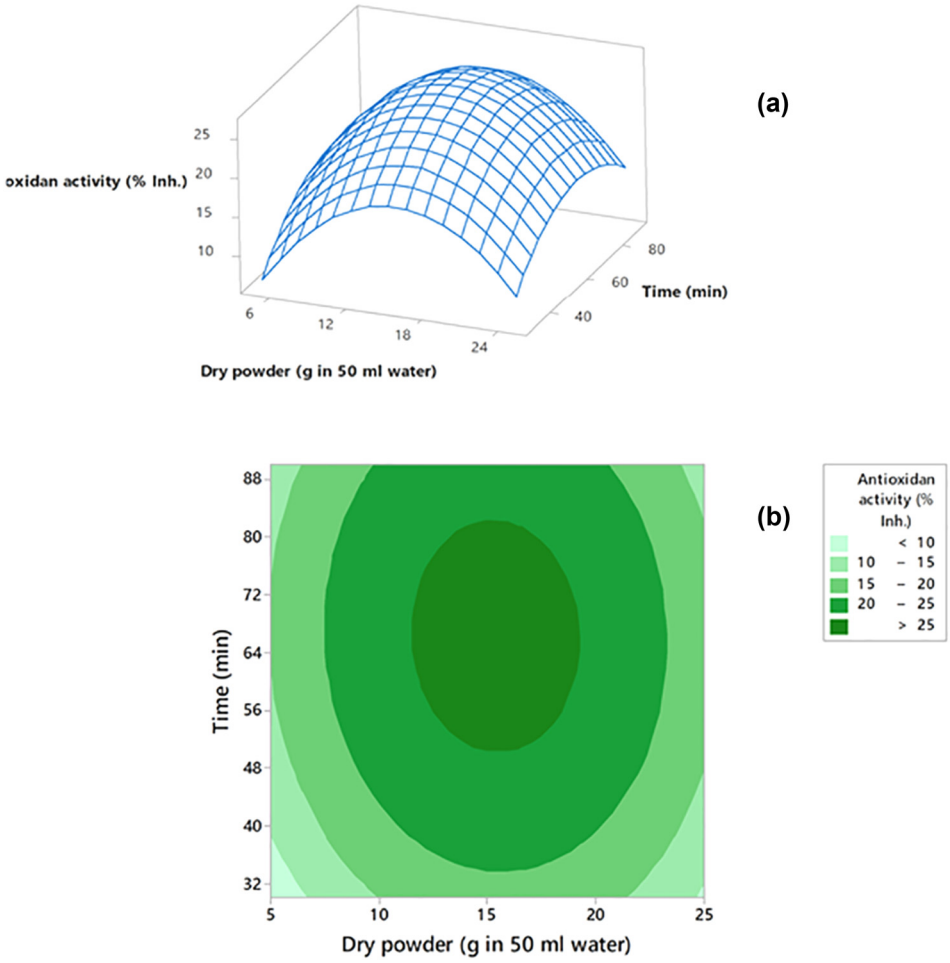

Figure 7: Response surface (a) and contour plots (b) for the antioxidant activity of the produced ZnO NPs.

the fabricated ZnO NPs as a result of the amount of dried powder and reaction time. As obviously shown in this figure, at a constant reaction time, by increasing the amount of dried powder, the antioxidant activities of the fabricated ZnO NPs increased and decreased. Nonetheless, the interaction of time of reaction and the amount of extract had insignificant ($p > 0.05$) effect on the antioxidant activity of the formed ZnO NPs. Regenerative agents increased by increasing the reaction time in the mixture solution containing constant amount of dried powder. However, extra heating time could destroy some regenerative agents and decrease antioxidant activity of the solution containing fabricated ZnO NPs [1]. The antioxidant activity of ZnO NPs might be because of the transmission of electron density situated at oxygen to the odd electron located at nitrogen atom in DPPH. This decreasing provides the proof regarding the free radical scavenging capacity of ZnO NPs and represented the creation of ZnO NPs. Also data showed that after the creation of ZnO NPs, by increment of concentration, their antioxidant activity was increased. The obtained results are the same line as the case of the previous findings by Madan et al. [12]. As clearly shown in Figure 7b, the maximum antioxidant activity was attained at the normal amount of dried powder and time of reaction.

3.4 Optimization of synthesis factors for the ZnO NPs fabrication

The ZnO NPs formation at the highest antioxidant and antibacterial inhibitory activities would be considered as an optimum product. For this purpose, the graphical optimization approach based on an overlaid contour plot was applied to discover the optimum region for the synthesis factors (Figure 8). The specified area of white color in Figure 8a show the desired time of reaction and the

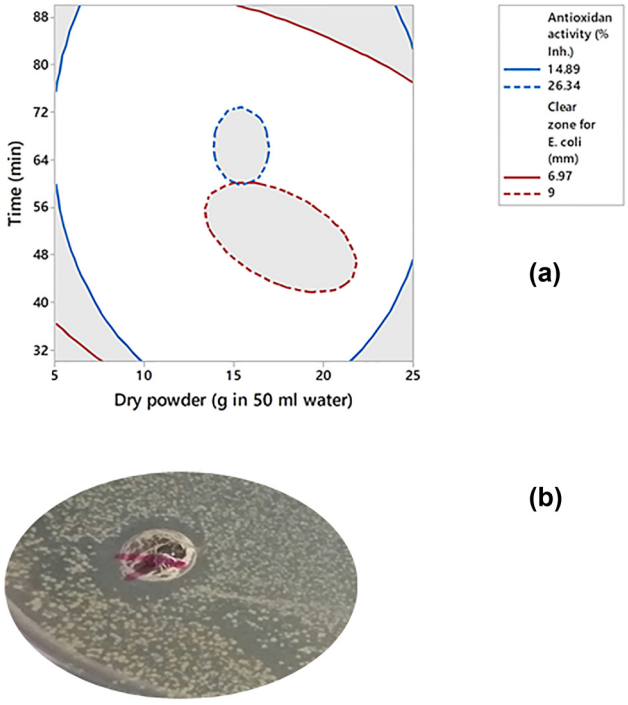

Figure 8: Overlaid contour plot of ZnO NPs as graphical optimization (a). Created clear zone in the plates amended with *E. coli* (b).

amount of dried powder to obtain the optimum ZnO NPs with highest antioxidant and antibacterial activities. Also for finding the exact optimum values of intentioned synthesis variables, a numerical multiple optimization was applied. The outcomes of the model validated that the fabrication conditions with 15.51 g of dried powder and 60 min fabrication reaction time for fabrication of the ZnO NPs. At the optimum conditions, ZnO NPs were fabricated with the antibacterial activity of 9 mm (zone of inhibition), as clearly shown in Figure 8b, and antioxidant of 26.36%. In addition, three experiments for the synthesis of ZnO NPs were prepared based on the recommended optimal values via numerical multiple optimization and characterized in terms of planned response variables. There was an insignificant difference among the experimental and predicted values of the optimum suggested sample, which was reaffirmation by the adequacy of the fitted models for examined responses.

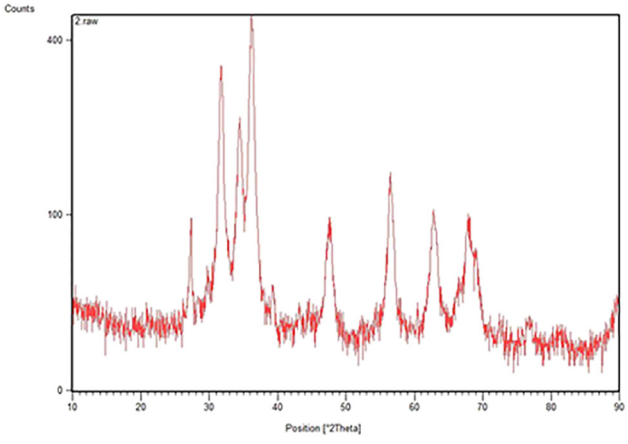

Figure 9: XRD pattern of the synthesized ZnO NPs at optimum conditions.

3.5 Physicochemical characteristics of the synthesized ZnO NPs at achieved optimum conditions

Figure 9 shows a typical X-rays diffraction (XRD) pattern of the optimized ZnO nanoparticles (λ = 1.5406 Å). Eight obtained Bragg peaks in (100), (002), (101), (102), (110), (103), (112), and (201) match completely with the single-phase ZnO wurtzite pattern (JCP 00-036-1451). The diffraction peaks detected at 2θ values are 31.74, 34.47, 36.22, 47.54, 56.55, 62.8, 67.94, and 69.10 (JPCDS card number: 36–1451), which showed the hexagonal phase of ZnO NPs. The lack of any additional peaks indicated that the pure crystalline ZnO NPs were fabricated [29]. The sharp peak was detected in (102) at 2θ = 36°. Their size of crystal was calculated via Debye–Scherrer formula (Eq. 3):

$$D = \frac{0.9\lambda}{\beta \cos \theta}. \quad (3)$$

The average crystal size of the sample was discovered to be 38 nm. A definite line broadening of the XRD peaks shows that the prepared material contains particles in the range of nanoscale. Obtained results were better than that of other studies related to green synthesized of ZNo NPs. Anvarinezhad et al. synthesized crystalline ZnO NPs using clove extract with a mean crystalline size of 50 nm [41]. Anzabi synthesized ZnO NPs using barberry extract with a mean crystalline size of 59 nm [42].

To assess the microstructure and shape of the formed ZnO NPs, a typical SEM image of the formed ZnO NPs was provided, which is shown in Figure 10. As observed, the formed NPs were finely dispersed with the similar structures. This similar shape point to that the formed NPs had not only least surface energy but also high thermodynamic stability, which authenticated the high value of the potential of zeta in the formed ZnO NPs. The configurations of SEM exhibited successful synthesis of triangular nanoprisms to approximately spherical with different size between 15 and 35 nm.

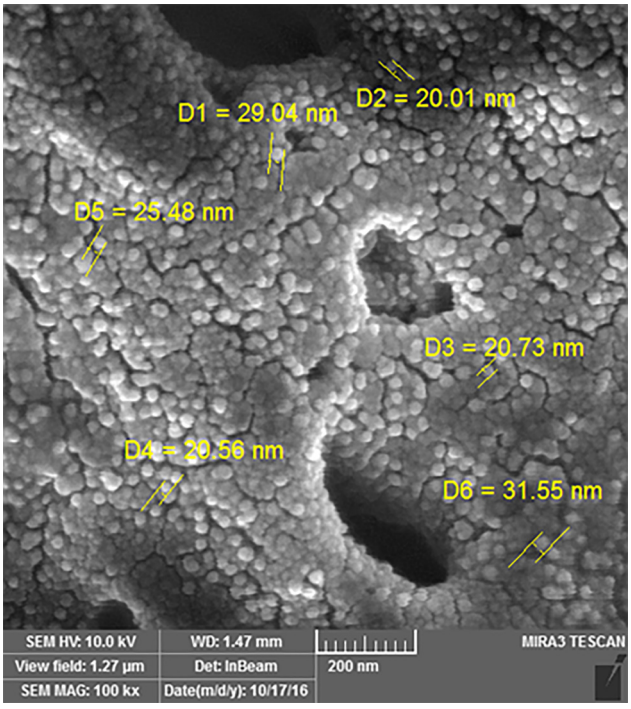

Figure 10: SEM images of the synthesized ZnO NPs at optimum conditions.

3.6 Antibacterial activity of films

Tables 5 and 6 present the results of the antibacterial activity of nanocomposite films against *E. coli* and *S. aureus*. Microplate reader recorded the absorbance of the samples before and after incubation. Minus sign indicates no growth of bacteria. While the wells containing polyethylene films (Sample 1) without ZnO NPs were opaque, which indicated the bacterial growth, those with ZnO NPs incorporated polyethylene films (Sample 2) were transparent that it showed no growth of bacteria. Wells containing polyethylene–starch films with ZnO NPs (Sample 3) slightly increased opacity that can be related to the release of starch, which microorganisms could use for its growth and reproduction.

4 Conclusions

The current study revealed that ZnO NPs can be synthesized using walnut leaf extract as regenerative agents (green method) without using any toxic chemicals. To our knowledge, this procedure has not been recently reported in the literature. The analysis by SEM displayed that the synthesized ZnO NPs were of small particle size with narrow size distribution. The results depicted the efficacy of RSM to study the effects of the conditions of synthesis on the dependent variables and to optimize them to achieve the most desirable ZnO NPs. The formed ZnO NPs and the ZnO NPs incorporated polyethylene films displayed significant antibacterial activity against *E. coli*.

Research funding: The authors state that no funding was involved.

Author contributions: Rouhina Saemi: founding, acquisition of data, analysis and interpretation of data, and original draft; Elham Taghavi: interpretation of data,

Table 5: Antibacterial inhibitory activity of films against *E. coli* before and after incubation

E. coli	S1	S1	S1	S2	S2	S2	S3	S3	S3	Control (+)	Control (–)
Before	0.0205	0.021	0.019	0.021	0.022	0.019	0.018	0.021	0.019	0.125	0.00025
After	0.2	0.197	0.198	0.018	0.02	0.018	0.034	0.04	0.039	0.261	0.0058
Difference	0.179	0.176	0.179	−0.003	−0.002	−0.001	−0.016	−0.0019	−0.02	0.136	0.00055

S – Sample.

Table 6: Antibacterial activity of films against *S. aureus* before and after incubation

S. aureus	S1	S1	S1	S2	S2	S2	S3	S3	S3	Control (+)	Control (–)
Before	0.019	0.0195	0.021	0.023	0.025	0.024	0.022	0.024	0.021	0.124	0.00025
After	0.211	0.202	0.199	0.022	0.021	0.021	0.028	0.03	0.027	0.215	0.0058
Difference	0.192	0.183	0.178	−0.001	−0.004	−0.003	0.006	0.006	0.006	0.091	0.00055

S – Sample.

original draft, review, and editing; Hoda Jafarizadeh-Malmiri: methodology, formal analysis, analysis and interpretation of data, review and editing, and supervision; Navideh Anarjan: study conception and design, interpretation of data, review and editing, and supervision.

Conflict of interest: The authors state no conflict of interest.

Data availability statement: All data generated or analyzed during this study are included in this published article.

References

[1] Khalil A, Ovais M, Ullah I, Ali M, Shinwari Z, Khamlich S, et al. Sageretia thea (Osbeck.) mediated synthesis of zinc oxide nanoparticles and its biological applications. Nanomedicine. 2017;12:1767–89.

[2] Hameed S, Khalil A, Ali M, Numan M, Khamlich S, Shinwari Z, et al. Greener synthesis of ZnO and Ag–ZnO nanoparticles using Silybum marianum for diverse biomedical applications. Nanomedicine. 2019;14:655–73.

[3] Horn D, Rieger J. Organic nanoparticles in the aqueous phase – theory, experiment, and use. Angew Chem Int Ed. 2001;40:4330–61.

[4] Kuppusamy P, Yusoff MM, Maniam GP, Govindan N. Biosynthesis of metallic nanoparticles using plant derivatives and their new avenues in pharmacological applications – an updated report. Saudi Pharm J. 2016;24:473–84.

[5] Dobrucka R, Długaszewska J. Biosynthesis and antibacterial activity of ZnO nanoparticles using Trifolium pratense flower extract. Saudi J Biol Sci. 2016;23:517–23.

[6] Elumalai K, Velmurugan S, Ravi S, Kathiravan V, Ashokkumar S. Bio-fabrication of zinc oxide nanoparticles using leaf extract of curry leaf (Murraya koenigii) and its antimicrobial activities. Mater Sci Semicond Process. 2015;34:365–72.

[7] Bano S, Nazir S, Nazir A, Munir S, Mahmood T, Afzal M, et al. Microwave-assisted green synthesis of superparamagnetic nanoparticles using fruit peel extracts: surface engineering, T2 relaxometry, and photodynamic treatment potential. Int J Nanomed. 2016;11:3833–48.

[8] Mohammadlou M, Jafarizadeh-Malmiri H, Maghsoudi H. Hydrothermal green synthesis of silver nanoparticles using Pelargonium/Geranium leaf extract and evaluation of their antifungal activity. Green Process Synth. 2017;6:31–42.

[9] Saranya S, Biosynthesis S. of gold nanoparticles (AuNPs) from C. orchioides and study their antimicrobial efficacy. Int J Phytopharm. 2015;5:58–64.

[10] Mayedwa N, Mongwaketsi N, Khamlich S, Kaviyarasu K, Matinise N, Maaza M. Green synthesis of zin tin oxide ($ZnSnO_3$) nanoparticles using Aspalathus Linearis natural extracts: structural, morphological, optical and electrochemistry study. Appl Surf Sci. 2018;446:250–7.

[11] Khalil AT, Ovais M, Ullah I, Ali M, Shinwari ZK, Hassan D, et al. Sageretia thea (Osbeck.) modulated biosynthesis of NiO nanoparticles and their in vitro pharmacognostic, antioxidant and cytotoxic potential. Artif Cell Nanomed Biotechnol. 2018;46:838–52.

[12] Sayyar Z, Jafarizadeh-Malmiri H. Preparation of curcumin nanodispersions using subcritical water–Screening of different emulsifiers. Chem Eng Technol. 2020;43:263–72.

[13] Ramesh M, Anbuvannan M, Viruthagiri G. Green synthesis of ZnO nanoparticles using Solanum nigrum leaf extract and their antibacterial activity. Spectrochim Acta A. 2015;136:864–70.

[14] Sawai J. Quantitative evaluation of antibacterial activities of metallic oxide powders (ZnO, MgO and CaO) by conductimetric assay. J Microbiol Methods. 2003;54:177–82.

[15] Upadhyaya L, Singh J, Agarwal V, Pandey AC, Verma SP, Das P, et al. In situ grafted nanostructured ZnO/carboxymethyl cellulose nanocomposites for efficient delivery of curcumin to cancer. J Polym Res. 2014;21:1–9.

[16] Sundrarajan M, Ambika S, Bharathi K. Plant-extract mediated synthesis of ZnO nanoparticles using Pongamia pinnata and their activity against pathogenic bacteria. Adv Powder Technol. 2015;26:1294–9.

[17] Albalawi MA, Eldiasty J, Khasim S, Badi N. Effect of Ag, Cu, and ZnO nanoparticle suspensions on the antimicrobial activity of tribulus terrestris herbal extracts. Nano Res. 2017;45:95–109.

[18] Eshun K, He Q. Aloe vera: a valuable ingredient for the food, pharmaceutical and cosmetic industries – a review. Crit Rev Food Sci Nutr. 2004;44:91–6.

[19] Iravani S, Korbekandi H, Zolfaghari B. Phytosynthesis of nanoparticles. In: Siddiqui MH, Al-Whaibi MH, Mohammad F, eds., Nanotechnology and plant sciences. Cham, Switzerland: Springer International Publishing; 2015. p. 203–58.

[20] Pereira JA, Oliveira I, Sousa A, Valentão P, Andrade PB, Ferreira ICFR, et al. Walnut (Juglans regia L.) leaves: phenolic compounds, antibacterial activity and antioxidant potential of different cultivars. Food Chem Toxicol. 2007;45:2287–95.

[21] Verma RS, Padalia RC, Chauhan A, Thul S. Phytochemical analysis of the leaf volatile oil of walnut tree (Juglans regia L.) from western Himalaya. Ind Crop Prod. 2013;42:195–201.

[22] Chaleshtori RS, Chaleshtori FS, Rafieian M. Biological characterization of Iranian walnut (Juglans regia) leaves. Turk J Biol. 2011;35:635–9.

[23] Sarker MAK, Rinta SK, Sayeed A. In vitro antioxidant and cytotoxic activities of the various extracts of Coccinia cordifolia leaves found in Bangladesh. Int J Pharmacogn Phytochem. 2016;5:260–3.

[24] Veiga R, Mendonça S, Mendes P, Paulino N, Mimica1 MJ, Lagareiro Netto AA, et al. Artepillin C and phenolic compounds responsible for antimicrobial and antioxidant activity of green propolis and Baccharis dracunculifolia DC. J Appl Microbiol. 2017;122:911–20.

[25] Amaral JS, Seabra RM, Andrade PB, Valentao P, Pereira JA, Ferreres F. Phenolic profile in the quality control of walnut (Juglans regia L.) leaves. Food Chem. 2004;88:373–9.

[26] Fukuda T, Ito H, Yoshida T. Antioxidative polyphenols from walnuts (Juglans regia L.). Phytochemistry. 2003;63:795–801.

[27] Chien S, Clayton W. Application of Elovich equation to the kinetics of phosphate release and sorption in soils. Soil Sci Soc Am J. 1980;44:265–8.

[28] Forino M, Stiuso P, Lama S, Ciminiello P, Tenore GC, Novellino E, et al. Bioassay-guided identification of the anti-hyperglycaemic constituents of walnut (Juglans regia) leaves. J Funct Foods. 2016;26:731–8.
[29] Azizi S, Ahmad MB, Namvar F, Mohamad R. Green biosynthesis and characterization of zinc oxide nanoparticles using brown marine macroalga Sargassum muticum aqueous extract. Mat Lett. 2014;116:275–7.
[30] Elumalai K, Velmurugan S. Green synthesis, characterization and antimicrobial activities of zinc oxide nanoparticles from the leaf extract of Azadirachta indica (L.). Appl Sur Sci. 2015;345:329–36.
[31] Thema F, Manikandan E, Dhlamini M, Maaza M. Green synthesis of ZnO nanoparticles via Agathosma betulina natural extract. Mater Lett. 2015;161:124–7.
[32] Salam HA, Sivaraj R, Venckatesh R. Green synthesis and characterization of zinc oxide nanoparticles from Ocimum basilicum L. var. purpurascens Benth.-Lamiaceae leaf extract. Mater Lett. 2014;131:16–8.
[33] Korbekandi H, Asghari G, Jalayer SS, Jalayer MS, Bandegani M. Nanosilver particle production using Juglans Regia L.(walnut) leaf extract. Jundishapur J Nat Pharm Prod. 2013;8:20–6.
[34] Anarjan N, Jafarizadeh-Malmiri H, Nehdi IA, Sbihi HM, Al-Resayes SI, Tan CP. Effects of homogenization process parameters on physicochemical properties of astaxanthin nanodispersions prepared using a solvent-diffusion technique. Int J Nanomed. 2015;10:1109–18.
[35] Anarjan N, Nehdi IA, Sbihi HM, Al-Resayes SI, Jafarizadeh-Malmiri H, Tan CP. Preparation of astaxanthin nanodispersions using gelatin-based stabilizer systems. Molecules. 2014;19:14257–65.
[36] Gharibzahedi SMT, Mousavi SM, Hamedi M, Razavi SH. Development of an optimal formulation for oxidative stability of walnut-beverage emulsions based on gum arabic and xanthan gum using response surface methodology. Carbohydr Polym. 2012;87:1611–9.
[37] Anarjan N, Jaberi N, Yeganeh-Zare S, Banafshehchin E, Rahimirad A, Jafarizadeh-Malmiri H. Optimization of mixing parameters for α-tocopherol nanodispersions prepared using solvent displacement method. J Am Oil Chem Soc. 2014;91:1397–405.
[38] Bezerra MA, Santelli RE, Oliveira EP, Villar LS, Escaleira LA. Response surface methodology (RSM) as a tool for optimization in analytical chemistry. Talanta. 2008;76:965–77.
[39] Nasrollahzadeh M, Maham M, Rostami-Vartooni A, Bagherzadeh M, Sajadid SM. Barberry fruit extract assisted in situ green synthesis of Cu nanoparticles supported on a reduced graphene oxide–Fe_3O_4 nanocomposite as a magnetically separable and reusable catalyst for the O-arylation of phenols with aryl halides under ligand-free conditions. RSC Adv. 2015;5:64769–80.
[40] Sheikhlou K, Allahyari S, Sabouri S, Najian Y, Jafarizadeh-Malmiri H. Walnut leaf extract-based green synthesis of selenium nanoparticles via microwave irradiation and their characteristics assessment. Open Agric. 2020;5:227–35.
[41] Anvarinezhad M, Javadi A, Jafarizadeh-Malmiri H. Green approach in fabrication of photocatalytic, antimicrobial, and antioxidant zinc oxide nanoparticles – hydrothermal synthesis using clove hydroalcoholic extract and optimization of the process. Green Process Synth. 2020;9:375–85.
[42] Anzabi Y. Biosynthesis of ZnO nanoparticles using barberry (Berberis vulgaris) extract and assessment of their physicochemical properties and antibacterial activities. Green Process Synth. 2018;7:114–21.